

Electronic structure of the $(\text{GaP})_1/(\text{InP})_1$ (111) strained-layer superlattice

Takeshi Kurimoto

NEC Scientific Information System Development, Ltd., 4-1-1 Miyazaki, Miyamae-ku, Kawasaki-shi, Kanagawa-ken 213, Japan

Noriaki Hamada

Fundamental Research Laboratories, NEC Corporation, 4-1-1 Miyazaki, Miyamae-ku, Kawasaki-shi, Kanagawa-ken 213, Japan and Department of Physics and Astronomy and Materials Research Center, Northwestern University, Evanston, Illinois 60201

(Received 20 October 1988; revised manuscript received 21 March 1989)

A first-principles all-electron band-structure calculation for $(\text{GaP})_1/(\text{InP})_1$ (111) monolayer superlattice reveals a novel band structure with a direct energy-band gap. The state at the bottom of the conduction band is strongly localized in the GaP layer, which is made from the states at the Γ and L points in bulk zinc-blende GaP. The state at the top of the valence band is weakly localized in the InP layer. The direct energy-band gap is smaller by 0.33 eV than the average of the gaps of bulk GaP and InP at the Γ point. We elucidate the relation between the energy band and the strain through a calculation of some auxiliary systems.

I. INTRODUCTION

Modern crystal-growth techniques such as molecular-beam epitaxy and metalorganic vapor-phase epitaxy (MOVPE) have made possible laboratory synthesis of ultrathin-layer superstructure. Among a variety of the superstructures, there is a special group of materials which spontaneously construct the superstructure under certain experimental conditions. One of them is the $(\text{GaP})_1/(\text{InP})_1$ monolayer superstructure in the [111] direction. Gomyo *et al.*¹ found that this system grown continuously by MOVPE exhibits an atomic ordering, which has recently been revealed to be the (111) monolayer superlattice by transmission electron microscopy,² and for which a formation mechanism has been proposed.³ This material has special importance if one considers the following points: It consists of GaP and InP, which have lattice constants that are very different from one another by 7.4%. It is a typical example of the ultrathin strained superlattice, with which we can study the relation between the band structure and the strain. The band gap of this superlattice is measured to be smaller by 80 meV than that of the disordered mixture,² which may be a result of the peculiar band structure of this superlattice.

We have performed a self-consistent band-structure calculation for the $(\text{GaP})_1/(\text{InP})_1$ (111) superlattice by using the all-electron full-potential linearized augmented-plane-wave (FLAPW) method⁴ within the local-density-functional formalism. In this paper, we will find that (i) this superlattice has a direct band gap; (ii) the charge density of the lowest conduction state is localized strongly in the GaP layer, and this state is made from the states at the Γ and L points of the bulk GaP; (iii) the highest valence state is weakly localized in the InP layer. We will discuss the origin of these features, and the relation between the strain and the band structure.

The organization of this paper is as follows. In Sec. II, we determine the lattice parameters of the superlattice

with the Keating model. In Sec. III, the band structure of the superlattice is presented. Section IV is devoted to a discussion of the relation between the band structure and the strain. We give a conclusion in Sec. V.

II. CRYSTAL STRUCTURE

It is important to determine the crystal structure carefully before starting to calculate the band structure, because the lattice parameters of bulk GaP and InP differ by as much as 7.4%, though these compounds have the same lattice type as zinc blende. In order to determine the lattice constants and the stable atomic positions in the superlattice, we employ the Keating model⁵ with two valence force constants of bond stretching and bond bending. The force constants have been set to fit the bulk elastic constants to the experimental values, and they are shown in Table I.

We start with the ideal zinc-blende lattice, and put Ga, In, and P atoms on the lattice to make the $(\text{GaP})_1/(\text{InP})_1$ monolayer superstructure in the [111] direction: the superlattice has a trigonal Bravais lattice associated with the point group C_{3v} , with space group $R3m$. Then, we change the lattice constants and the atomic positions according to the forces provided by the Keating model. Finally, we obtained the stable structure, which is shown as system C in Table II and Fig. 1(a). Though the superlat-

TABLE I. Parameters in the Keating model: r is the equilibrium interatomic distance, α the bond-stretching force constant, and β the bond-bending force constant. The bond-bending force constant for Ga—P—In is assumed to be the arithmetic mean of β 's in this table. (1 Ry = 13.6058 eV, 1 a.u. = 0.529 177 Å.)

	r (a.u.)	α (mRy/a.u. ²)	β (mRy/a.u. ²)
GaP	4.461	57.13	14.96
InP	4.802	51.33	9.92

TABLE II. Crystal structures used for the band-structure calculations. The values are referred to the hexagonal basis set. System *C* is the superlattice determined by the Keating model. $\frac{1}{24}=0.04166$, $\frac{1}{6}=0.16666$, and $\frac{5}{24}=0.20833$. $c=a\sqrt{24}$ for *A*, *D*, and *E* systems. The cubic lattice parameters for system *A* are 10.3012 a.u. for GaP and 11.0900 a.u. for InP.

System	GaP	<i>A</i>	InP	<i>B</i>	<i>C</i>	<i>D</i>	GaP	<i>E</i>	InP
$a=b$ (a.u.)	7.2840	7.8418	7.8418	7.5110	7.5110	7.5110	7.5110	7.5110	7.5110
c (a.u.)	35.6844	38.4169	38.4169	37.1166	37.2640	36.7962	36.7962	36.7962	36.7962
	z coordinate for atomic positions								
Ga	0			0.0	0.0	0	0		
P(I)	$\frac{1}{24}$			0.0282	0.0371	$\frac{1}{24}$	$\frac{1}{24}$		
In		0.0		0.1576	0.1659	$\frac{1}{6}$			0
P(II)		$\frac{1}{24}$		0.2131	0.2137	$\frac{5}{24}$			$\frac{1}{24}$

tice has a trigonal Bravais lattice, we refer to the corresponding hexagonal axes as usual. The length of the c axis corresponds to the double of the body diagonal of the cubic cell. The length of a and b axes corresponds to a half of the face diagonal of the cubic cell.

The determined superlattice which is referred to as sys-

tem *C* has the following features. (i) The lateral lattice constant, a , shrinks by 0.7% compared with the average one (7.5629 a.u.) of the constituent compounds. (ii) The c/a ratio is 4.9613, which is elongated from the ideal value, $\sqrt{24}=4.8990$. As a result, the volume of the unit cell is smaller than the average one of the constituent compounds by 0.8%. (iii) Ga—P and In—P bond lengths in the c direction are similar to those of the constituent compounds within 0.1%, while (iv) lateral bonds near the superlattice plane are elongated by 2.0% for Ga—P, and are shortened by 2.4% for In—P compared with those of the constituent compounds, respectively.

For the purpose of further elucidating the feature of the above superlattice determined with the Keating model, we will also treat two auxiliary superlattices: One, which is referred to as system *D*, is that in which the a and b axes are the same as those of the above superlattice, while the c/a ratio takes the ideal value ($\sqrt{24}$), and all the bond lengths are exactly the same; the other system, which is referred to as system *B*, is that in which the a and b axes are the same as the previous ones, while the Ga—P and In—P bond lengths coincide with the bulk values of the constituents, respectively. In Table II, we summarize the systems treated in this paper, together with the pure compounds. System *A* contains the pure GaP and InP with experimental lattice parameters. System *E* contains the pure compounds with the same lattice parameters as in system *D*. Table III shows the extent of the strain of each system by presenting the deviation of the bond length from the bulk values.

The Brillouin zone of the superlattice is shown in Fig.

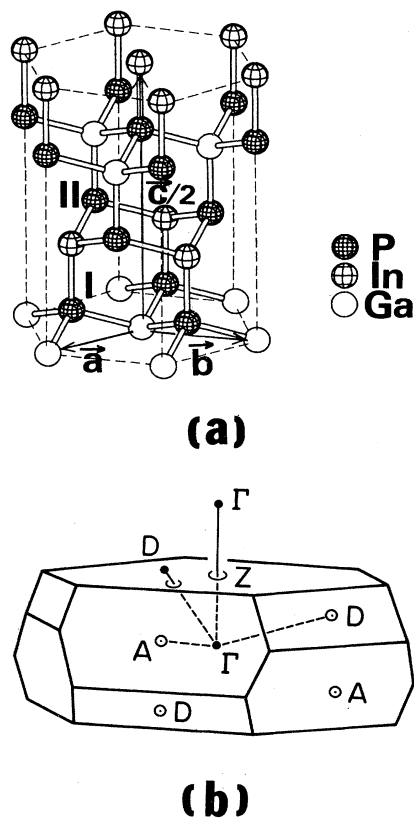


FIG. 1. (a) The crystal structure of the superlattice, which has a trigonal Bravais lattice. The crystal axes are shown for the hexagonal lattice, which are referred to represent the positions of atoms in Table II. It has two kinds of phosphorus atoms: one, P(I), makes the staggered honeycomb layers together with Ga, which are called GaP layers, and the other, P(II), makes InP layers. (b) The first Brillouin zone and the high-symmetry points.

TABLE III. Deviation of the bond length from the bulk bond length. Ga—P(I) bonds construct the GaP layer and In—P(II) bonds construct the InP layer. Ga—P(II) and In—P(I) bonds have a direction parallel to the c axis of the hexagonal coordination system.

System	<i>A</i> (%)	<i>B</i> (%)	<i>C</i> (%)	<i>D</i> (%)	<i>E</i> (%)
Ga—P(I)	0	0.0	2.0	3.1	3.1
Ga—P(II)	0	0.0	-0.08	3.1	3.1
In—P(I)	0	0.0	-0.08	-4.2	-4.2
In—P(II)	0	0.0	-2.4	-4.2	-4.2

1(b). The correspondence of the high-symmetry points between the superstructure and the zinc-blende structure is as follows: Γ corresponds to Γ and L , D to L and X , and Z to the halfway point on the line of $\Gamma-L$.

III. RESULTS

Self-consistent band-structure calculations have been performed by using the all-electron FLAPW method,⁴ in which the linearization is done with the scheme of Take-da and Kübler.⁶ Ga $3d$ and In $4d$ electrons are treated as the core electrons, which are relaxed fully in the self-consistent procedure.

The energy-band structure of system *C* is shown in Fig. 2. It has a direct band gap of 0.73 eV at the Γ point. The band structure is drawn along the line of $Z-\Gamma-D-\Gamma$, where the line $\Gamma-D$ goes from the first Brillouin zone to the second one through the upper hexagon in Fig. 1(b), and the last Γ sits at the center of the second Brillouin zone. This line corresponds to the lines of $(\Gamma L/2)-\Gamma-X-L$ and $(\Gamma L/2)-L-L-\Gamma$ in the zinc-blende (fcc) structure, where $(\Gamma L/2)$ stands for the half-way point on the line $\Gamma-L$. In order to elucidate this correspondence, we show the band structures of bulk GaP and InP in Fig. 3, where the states are identified in terms of the high-symmetry points in the fcc Brillouin zone. By comparing Fig. 2 with Fig. 3, we can often identify the states of the superlattice approximately by the special points in the fcc Brillouin zone. Examples of such identification are shown in Fig. 2.

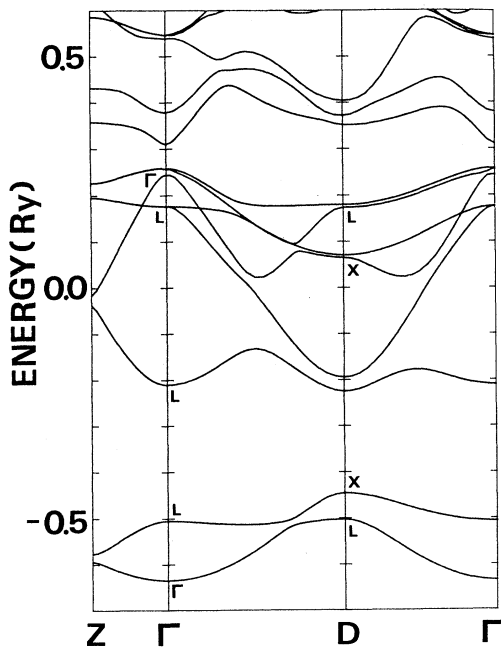


FIG. 2. Energy-band structure for the superlattice of system *C*, which has the structure determined by the Keating model. The letters Γ , L , and X inside the figure show the approximate identification in terms of the high-symmetry points of the zinc-blende Brillouin zone.

Figure 4 shows the charge density of the state at the top of the valence band. It is mainly made of the $3p$ states of P, as is generally seen at the valence-band top in the III-V compounds. It has larger weight in the InP layer than in the GaP layer, which implies that the potential of the InP layer is higher than that of the GaP layer.

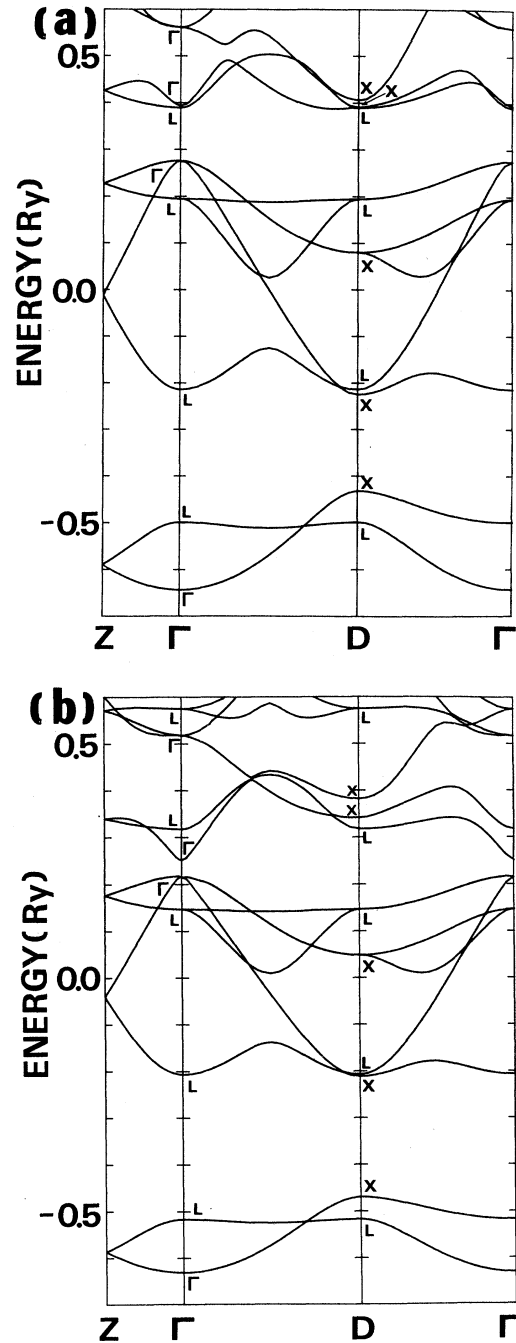


FIG. 3. Energy-band structures for the bulk (a) GaP and (b) InP of system *A* that are folded into the trigonal Brillouin zone. The letters Γ , L , and X inside the figure show the identification in terms of the high-symmetry points of the zinc-blende Brillouin zone.

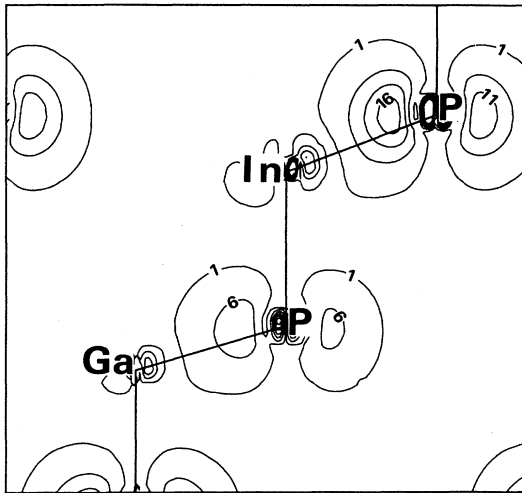


FIG. 4. The charge density of the topmost valence state at the Γ point for the superlattice of system *C* in units of 10^{-3} e/a.u.³ Contours are drawn in a plane perpendicular to the layer, and are spaced in increments of 0.005 e/a.u.³ with the smallest of 0.001 e/a.u.³

The lowest two states of the conduction band at the Γ point has a special character. Those states cannot be identified by a certain point in the zinc-blende Brillouin zone; instead, they can be characterized by a strong localization. The lowest state is strongly localized in the GaP layer, while the second lowest state is strongly localized in the InP layer. The first lowest state is a mixture of the lowest conduction states at the Γ and L points of GaP. In order to explain this point, the charge densities of them are shown in Fig. 5. The states of bulk GaP at the Γ and L points are mainly made of the s states of Ga and P, as are shown in Figs. 5(b) and 5(c) and Table IV (a): The state at the Γ point has an antibonding character at every bond, while the state at the L point has an antibonding character within a layer and has a weak bonding character between the layers. When these two states are superposed, the resulting state is localized in every two layers. This superposed state becomes the lowest conduction state at the Γ point of the superlattice, as is shown in Fig. 5(a). Generally speaking, the wave function at the Γ point essentially has a functional form of 1, while the wave function at the L point has the functional form of $\exp(i\pi z/d)$ or $\exp(-i\pi z/d)$ in the direction of (111) in the fcc lattice, where z stands for the position of (111) direction, and d is the interlayer spacing ($d=c/6$). The superposed state essentially has a functional form of $1 + \cos(\pi z/d)$, which is localized in every two layers. The second lowest conduction state at the Γ point has a similar feature, which is localized in the InP layers.

The calculated direct gaps at the Γ point are 0.73 eV for the superlattice, and 1.62 and 0.50 eV for bulk GaP and InP, respectively. Therefore, the band gap of the superlattice is much smaller by 0.33 eV than the average of these bulk direct gaps. In the next section, we will show the reason why the direct gap becomes so small.

IV. DISCUSSION

We have performed the self-consistent band-structure calculation also for all the other systems in Table II with the same condition as in Sec. III. In Fig. 6, we compare some energy levels at the Γ point for all the systems from *A* to *E*. The reference energy level is taken at the average of the P 1s core levels for each system. The core levels in systems *B* and *D* are assumed to coincide with those in systems *A* and *E*, respectively. This choice for the reference of energy has been shown to be appropriate for the estimation of the valence-band offset in AlAs/GaAs superlattices.^{7,8} In the case of the ultrathin superlattice, this choice is rather artificial, but it gives us a reasonable viewpoint for the interpretation of the level scheme. In this section, we will elucidate the effect of the strain on the band structure and look at Fig. 6 in detail. In the following discussion, we shall keep it in mind that the strain of the bond length becomes larger in going from system *A* to system *E*.

The valence-band top of InP is much higher in energy than that of GaP in system *A*, while they are almost the same in system *E*. We "define" the valence-band offset of system *B* as the difference of the valence-band tops of GaP and InP in system *A*, and the valence-band offset of system *D* as that in system *E*. Then, the valence-band offsets are 0.92 eV for system *B* and 0.00 eV for system *D*. The valence-band offset of system *C* is inferred as about 0.3 eV from Fig. 6. This estimation has no strict meaning quantitatively, but it is helpful in order to understand the feature of the valence band. For example, this change of the valence-band offset from system *B* to *D* coincides with the change of the extent of the localization of the highest valence-band state as seen in Table V. This change is related to the change of the electron number inside the muffin-tin spheres, which is shown in Fig. 7.

The conduction-band bottom is dominated by the GaP state, as has been seen for system *C* in the preceding section. This is the case for all the systems in Fig. 6; therefore, this fact can be true generally for the system consisting of GaP and InP. However, it does not mean that the strain is not important; instead, it is instructive to know that the band gap of GaP in system *E* is much smaller than the gap in system *A*, while the situation is opposite for InP. If there was not this change of the band gap, the lowest conduction band would be localized in the InP layer in systems *C* and *D*.

In the previous section, we found that the band gap of the superlattice is 0.33 eV smaller than the average of the bulk direct gaps. By comparison, we cite several experiments. The direct gaps at 300 K are 2.77 and 1.34 eV for bulk GaP and InP, respectively,⁹ which are much (~ 1 eV) larger than the calculated values. This large discrepancy, which comes from the local-density approximation used in our calculation, is, however, resolved by simply shifting the conduction bands rigidly upwards relative to the valence bands. For simple semiconductors such as Si,¹⁰ Ge,¹⁰ AlAs,¹¹ and GaAs,¹¹ it has been shown by a field-theoretical calculation that the local-density approximation provides good wave functions for the valence and the conduction bands, and that the self-energy corrections primarily give rigid energy shifts of

the valence and the conduction bands. Though the self-energy correction for the superlattice is not known yet, we can expect that the self-energy correction smoothly varies from state to state, and, especially for the ultrathin superlattice, it is not much different from those of the constituent materials because the self-energy correction is predominately determined by the dielectric property of

the material. Therefore, we believe that the comparison of the relative changes of band gaps on making the superlattice is meaningful in our calculation using the local density approximation. To begin with, the optical bowing for the disordered 50% mixed crystal of GaP and InP is measured⁹ to be 0.19 eV by cathodoluminescence and photoluminescence. A further reduction of the band gap

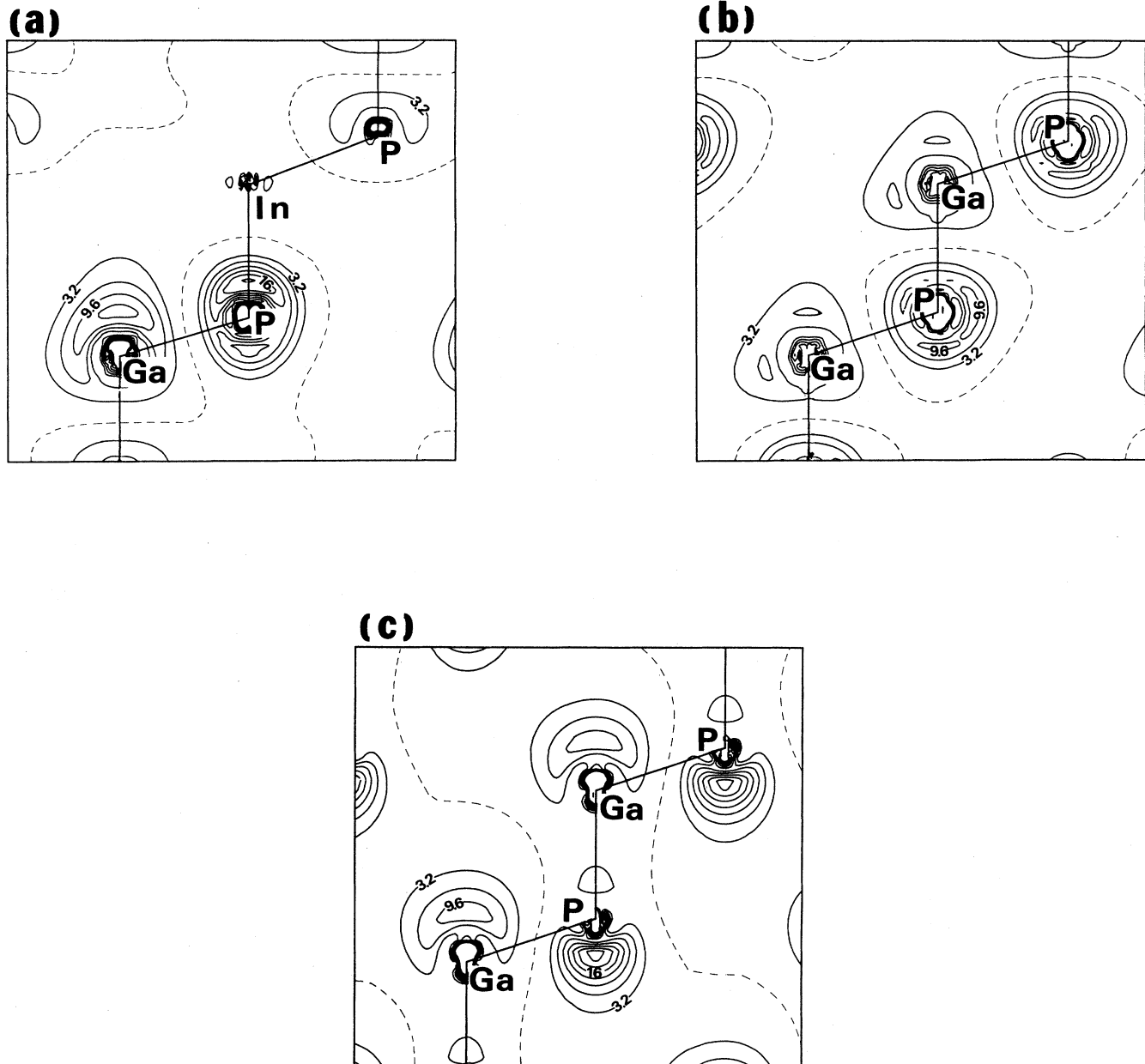


FIG. 5. The charge densities of the lowest conduction states (a) at the Γ point for the superlattice of system C, (b) at the Γ point, and (c) at L point for the bulk GaP of system A in units of $10^{-3} e/a.u.^3$. Contours are equally spaced in increments of $0.0032 e/a.u.^3$. The smallest value of the contour, shown by the dashed line, is zero, which corresponds to the node of the wave function.

TABLE IV. Projected weights of the (a) lowest and (b) second lowest conduction states into the *s* and *p* states in the muffin-tin spheres.

System		A		(a)			E	
		GaP (Γ)	GaP(L)	B	C	D	GaP(Γ)	GaP(L)
Ga	4s	0.340	0.260	0.244	0.271	0.284	0.368	0.258
	4p	0.0	0.038	0.021	0.008	0.004	0.0	0.044
P(I)	3s	0.406	0.172	0.211	0.262	0.272	0.386	0.158
	3p	0.0	0.044	0.049	0.002	0.009	0.0	0.058
In	5s			0.030	0.045	0.027		
	5p			0.003	0.002	0.006		
P(II)	3s			0.062	0.075	0.056		
	3p			0.041	0.009	0.005		

System		A		(b)			E	
		InP(Γ)	InP(L)	B	C	D	InP(Γ)	InP(L)
Ga	4s			0.017	0.031	0.017		
	4p			0.067	0.036	0.012		
P(I)	3s			0.000	0.004	0.001		
	3p			0.013	0.013	0.019		
In	5s	0.294	0.240	0.202	0.198	0.223	0.244	0.238
	5p	0.0	0.042	0.002	0.003	0.016	0.0	0.032
P(II)	3s	0.360	0.152	0.181	0.190	0.221	0.382	0.170
	3p	0.0	0.048	0.079	0.047	0.013	0.0	0.032

TABLE V. Projected weight of the three highest valence states [(a) the twofold highest valence state and (b) the second-highest valence state] into the *s* and *p* states in the muffin-tin spheres.

System		A		(a)			E	
		GaP	InP	B	C	D	GaP	InP
Ga	4s	0.0		0.0	0.0	0.0	0.0	
	4p	0.086		0.002	0.018	0.034	0.078	
P(I)	3s	0.0		0.0	0.0	0.0	0.0	
	3p	0.544		0.077	0.184	0.254	0.530	
In	5s		0.0	0.0	0.0	0.0		0.0
	5p		0.056	0.053	0.045	0.035		0.062
P(II)	3s		0.0	0.0	0.0	0.0		0.0
	3p		0.532	0.464	0.362	0.290		0.556

System		A		(b)			E	
		GaP	InP	B	C	D	GaP	InP
Ga	4s	0.0		0.060	0.006	0.000	0.0	
	4p	0.086		0.006	0.027	0.038	0.078	
P(I)	3s	0.0		0.072	0.009	0.000	0.0	
	3p	0.544		0.238	0.280	0.264	0.530	
In	5s		0.0	0.001	0.001	0.000		0.0
	5p		0.056	0.042	0.042	0.032		0.062
P(II)	3s		0.0	0.002	0.002	0.000		0.0
	3p		0.532	0.184	0.238	0.279		0.556

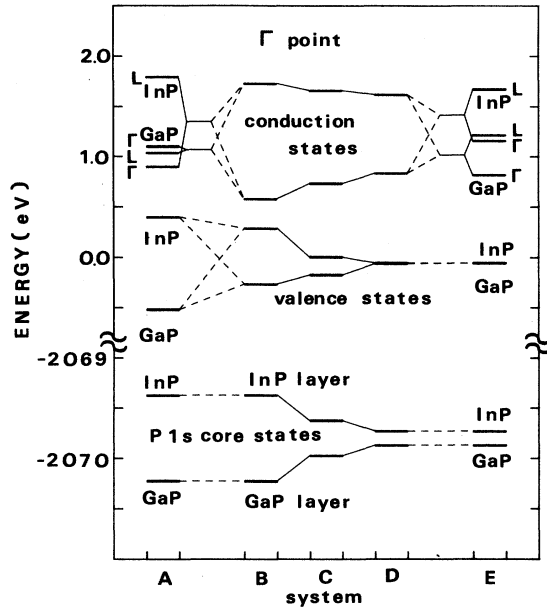


FIG. 6. Energy levels at the Γ point for systems $A-E$. The averages of the $1s$ core levels of P for each system are lined up. The $1s$ core levels of P for systems A and E are assumed to coincide with the corresponding levels for systems B and D . The topmost level of the valence band is twofold for the superlattices ($B-D$) and is threefold for the pure systems (A and E).

due to the superlattice ordering is measured² recently as 0.08 eV by photoluminescence. Thus, the band gap of the superlattice is smaller than the average of the bulk direct gaps experimentally by 0.27 eV, which should be compared with our value of 0.33 eV. The agreement should be considered to be very good considering the uncertainty of quantities involved. Experimentally, the extent of the ordering has not been measured, and the recombination processes in luminescence are not clear yet. On the other hand, the theory uses the local-density approximation, and contains some uncertainty in crystal-structure parameters. In the context of the local-density approximation, the self-energy correction should be considered in the future for the definite conclusion about the band gaps and the details of the band structure.

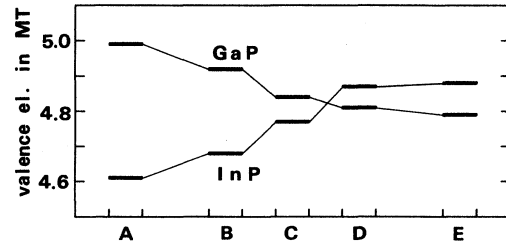


FIG. 7. The numbers of valence electrons inside the muffin-tin spheres in the GaP and InP layers.

V. CONCLUSION

A first-principles band-structure calculation by the FLAPW method has been done for the $(\text{GaP})_1/(\text{InP})_1$ (111) superlattice and related systems. We have found that (i) the superlattice has a direct band gap, which is smaller by 0.33 eV than the average gap of the constituent bulk compounds at the Γ point; (ii) the charge density of the lowest conduction state is localized strongly in the GaP layer; (iii) the lowest conduction state is made from the states at the Γ and L points of the bulk GaP; (iv) the highest valence state is weakly localized in the InP layer. We have also found that the valence-band offset and the band gap change very much with strain. We have determined the stable structure of the superlattice by using the Keating model, which is expected to be sufficiently near to fact. The above qualitative conclusion does not change within reasonable changes in the structure parameters.

ACKNOWLEDGMENTS

We would like to express our thanks to Dr. T. Suzuki, Dr. A. Gomyo, and Dr. S. Iijima for fruitful discussions on their experiment. Thanks are also due to Dr. A. Oshiyama, Dr. M. Saito, Dr. S. Ohnishi, Professor K. Terakura, and Professor A. J. Freeman for their helpful discussions on the theoretical and computational aspects, and to Professor A. Yanase for providing us with the computer-graphics program. The numerical calculations have been performed using the NEC SX-2 supercomputer in the NSIS Computer Center.

¹A. Gomyo, K. Kobayashi, S. Kawata, I. Hino, T. Suzuki, and T. Yuasa, *J. Cryst. Growth* **77**, 367 (1986); A. Gomyo, T. Suzuki, K. Kobayashi, S. Kawata, I. Hino, and T. Yuasa, *Appl. Phys. Lett.* **50**, 673 (1987).

²A. Gomyo, T. Suzuki, and S. Iijima, *Phys. Rev. Lett.* **60**, 2645 (1988).

³T. Suzuki, A. Gomyo, and S. Iijima, *J. Cryst. Growth* **93**, 396 (1988).

⁴E. Wimmer, H. Krakauer, M. Weinert, and A. J. Freeman, *Phys. Rev. B* **24**, 864 (1981); H. J. F. Jansen and A. J. Freeman, *ibid.* **30**, 561 (1984).

⁵P. N. Keating, *Phys. Rev.* **145**, 637 (1966).

⁶T. Takeda and J. Kübler, *J. Phys. F* **9**, 661 (1979).

⁷S. Massidda, B. I. Min, and A. J. Freeman, *Phys. Rev. B* **35**, 9871 (1987).

⁸S.-H. Wei and A. Zunger, *Phys. Rev. Lett.* **59**, 144 (1987).

⁹A. Onton, M. R. Lorenz, and W. Reuter, *J. Appl. Phys.* **42**, 3420 (1971).

¹⁰M. S. Hybertsen and S. G. Louie, *Phys. Rev. B* **34**, 5390 (1986).

¹¹R. W. Godby, M. Schlüter, and L. J. Sham, *Phys. Rev. B* **35**, 4170 (1987).